# Stress-dependent susceptibility of Galfenol and application to force sensing

P. G. Evans[1,a)] and M. J. Dapino[2,b)]
[1]*Lincoln Laboratory, Massachusetts Institute of Technology, Lexington, Massachusetts 02420, USA*
[2]*Department of Mechanical Engineering, The Ohio State University, Columbus, Ohio 43210, USA*

(Received 25 August 2009; accepted 3 August 2010; published online 12 October 2010)

A sensing principle, operating regime, and composition range are identified for force sensing with Galfenol alloys. Magnetization measurements of $Fe_{79.1}Ga_{20.9}$ and $Fe_{81.6}Ga_{18.4}$ are performed under applied magnetic field at constant stress. Stress-dependent, linear regions with negligible hysteresis are observed in the $Fe_{79.1}Ga_{20.9}$ sample over a large range of fields and stresses, for which an analytic model for unbiased loops is formulated. Similar regions are observed in the $Fe_{81.6}Ga_{18.4}$ sample, with a more limited stress and field range. The small signal operating regime (small in field, not in stress) centered about zero magnetic field is particularly advantageous because in this regime there is no observable hysteresis, since the magnetization process occurs by domain rotation only. The measurements and model show that in this region the susceptibility of $Fe_{79.1}Ga_{20.9}$ is more sensitive to stress (owing to a significantly lower fourth-order anisotropy constant) with only a small reduction in the saturation magnetization and magnetostriction as compared to $Fe_{81.6}Ga_{18.4}$. For force sensing, these results suggest the use of Galfenol with an ideal Ga content in the range of 19–22 at. % in which a small, positive fourth-order anisotropy constant is obtained, though in this composition range the magnetostriction is sacrificed. © *2010 American Institute of Physics*.
[doi:10.1063/1.3486019]

## I. INTRODUCTION

Magnetostrictive materials exhibit dimensional changes in response to magnetic fields and magnetization changes in response to applied stresses. These effects have been used to create actuators and sensors which in some cases deliver superior performance with less weight, size, and moving parts than traditional electromagnetic devices.[1] Iron–gallium alloys (Galfenol) are an emerging class of magnetostrictive materials which have moderate magnetostriction ($\sim 400 \times 10^{-6}$) and steel-like structural properties.[2] Prior to the advent of Galfenol, the choice of magnetostrictive materials was restricted to mechanically robust materials with low magnetostriction such as iron and nickel or brittle materials with large magnetostriction such as Terfenol-D ($Tb_yDy_{1-y}Fe_x$). The unique combination of mechanical robustness and high magnetostriction of Galfenol makes it ideal for creating sensors and actuators that can take tension, bending, torsion, and shock loads in harsh environments. Furthermore, Galfenol can be machined, welded, and deposited into complex geometries.

Models are used to describe nonlinear behavior in the design and control of magnetostrictive devices.[3] Jiles and Thoelke[4] employed energy minimization to quantify the effect of stress and anisotropy on the magnetization of Terfenol-D. Their model incorporates the underlying assumptions present in the Stoner–Wohlfarth (SW) model and its derivatives. The magnetization is calculated as the sum of the contributions of a set of noninteracting rotational particles or domains where rotation is induced by an applied field or stress. The orientation of the domains is calculated from the minimization of the anisotropy, field, and magnetostrictive energies. This model has instantaneous jumps as minima are eliminated and created at certain critical fields and stresses. While the sharp transitions in their approach do not agree with measurements, the model provides an overall description of the magnetization mechanism.

In Armstrong's hysteretic model for magnetostrictive materials,[5] magnetization is also attributed to a discrete set of domains but in this model the domains do not rotate. This assumption can be made when the anisotropy energy is high and the field and stress are applied along one of the preferred crystal directions dictated by the anisotropy energy. Magnetization and magnetostriction changes occur as the fractional occupancies of the domains in the set change. These changes are calculated from energy principles.

Other models for magnetostrictive materials use statistical mechanics to smooth sharp transitions predicted by direct energy minimization. Smith and Dapino[6] applied stochastic homogenization in conjunction with direct energy minimization to model the effect of stress on magnetization of a variety of ferromagnetic materials. The energy includes thermal, exchange, stress, and magnetic field terms but not anisotropy. Stochastic homogenization smoothes the sharp transitions predicted by energy minimization by treating the critical field at which a transition occurs as a statistically distributed parameter.

Statistical mechanics principles have also been used to characterize the effect of stress annealing and to model rate-dependent hysteresis in Galfenol.[7,8] In these models, any domain orientation is possible; the likelihood of a given domain orientation is calculated from the energy of the orientation,

[a)]Electronic mail: phillip.evans@ll.mit.edu.
[b)]Electronic mail: dapino.1@osu.edu.

 

which incorporates anisotropy, stress, and magnetic field terms. The energy is not directly minimized but the probability density function causes minimum energy orientations to be more likely. In micromagnetics models, the energy is minimized over a geometry with boundary conditions.[9] While these models provide more detailed information such as domain structure they are computationally expensive and better suited for material design and characterization rather than device design and control.

Chief intent of this study is to identify a force sensing principle, operating regime, and composition range for design of Galfenol force sensors. Magnetization measurements of $Fe_{79.1}Ga_{20.9}$ and $Fe_{81.6}Ga_{18.4}$ are performed under applied magnetic field at constant stress. Energy minimization is used to interpret the difference in the magnetization process for the two samples. A simple analytical model is derived for the field and stress dependence of the linear region appearing in magnetization measurements of ⟨100⟩ oriented Galfenol, obtained from varying the magnetic field at constant stress. Magnetization changes in this region are attributed to domain rotation and the domain orientation is found from the Gibbs free energy of a SW particle. Using this simple model it is shown that, because of its lower anisotropy, Galfenol with higher Ga content is ideal for transducers operating on the principle of stress dependent susceptibility. Furthermore, it is shown that although the stress dependence of the susceptibility is nonlinear, a linear force sensor can be constructed using a transformer with a Galfenol element. A similar model[10] has been developed for amorphous magnetostrictive sensors but this model does not apply to materials with cubic anisotropy.

## II. MEASUREMENTS

Magnetization measurements are reported for ⟨100⟩ oriented, single-crystal $Fe_{79.1}Ga_{20.9}$ and ⟨100⟩ oriented, textured polycrystal $Fe_{81.6}Ga_{18.4}$. The textured polycrystal is near single-crystalline with 95% of grains having the ⟨100⟩ axis aligned within 5° of the rod axis. Prior to magnetic field application, a constant bias stress is applied with an MTS 858 table top system capable of applying compressive loads only, by loading the sample between two parallel plates. A cyclic magnetic field is then applied using a drive coil situated with the Galfenol sample in a steel canister providing a flux return path. The waveform is triangular with a rate of 1 kA/m per second and magnitude sufficient to saturate the sample. The magnetic field is measured on the surface of the rod halfway along its length with a Lakeshore 421 gauss meter and magnetic flux density is measured with a Walker Scientific MF-30 fluxmeter and pick-up coil. Magnetization is calculated by subtracting the field measurements from flux density measurements. Prior to saturation, linear regions are observed in the magnetization versus field curves of the single-crystal sample (see Fig. 1) where the slope depends on the bias stress. The sample with lower Ga content also has linear regions but exhibits significant kinking with a nonlinear shape prior to saturation.

In Sec. III, an analytical model is developed for the slopes of these linear and anhysteretic regions of the measurements. The model describes domain rotation and is applicable to the linear, anhysteretic regions only. The model accurately describes the nonlinear dependence of the slope or susceptiblity of these regions on stress. Additionally, it shows that the difference in behavior of $Fe_{79.1}Ga_{20.9}$ and $Fe_{81.6}Ga_{18.4}$ is due to a difference in the anisotropy. Utilizing this model, equations for the operation of a linear magnetoelastic force sensor are derived in Sec. IV.

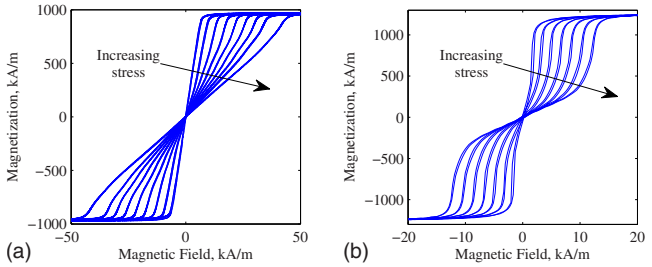


FIG. 1. (Color online) Magnetization measurements of (a) $Fe_{79.1}Ga_{20.9}$ at constant compressive stresses of 1.38, 18.8, 27.6, 41.4, 55.2, 68.9, 82.7, 96.5, and 122.7 MPa; (b) $Fe_{81.6}Ga_{18.4}$ at constant compressive stresses of 0.316, 9.17, 18.5, 27.7, 36.9, 46.2, and 55.4 MPa.

## III. MAGNETIZATION MODEL

Ferromagnetic materials are composed of regions of uniform magnetization $M_s$ called domains.[11] Magnetization changes occur as domains rotate or as differently orientated domains change size through domain wall motion. In the SW approximation used here, the material is taken as a collection of noninteracting, single-domain particles.[12] This approximation is accurate when domain rotation is the dominant magnetization mechanism; domain rotation is modeled as the rotation of SW particles. The orientation $\mathbf{m}$ of an SW particle can be calculated from its Gibbs free energy $G$ which has natural dependence on the applied quantities magnetic field $\mathbf{H}$, stress $\mathbf{T}$, and temperature $\theta$ as well as the internal state variable $\mathbf{m}$. The Gibbs free energy $G$ is the sum of the anisotropy

$$G_{an} = K_4(\theta)(m_1^2m_2^2 + m_2^2m_3^2 + m_3^2m_1^2) + K_6(\theta)m_1^2m_2^2m_3^2, \quad (1)$$

Zeeman

$$G_z = -\mu_0 M_s(\theta)\mathbf{m}\cdot\mathbf{H}, \quad (2)$$

magnetomechanical coupling

$$G_{coup} = -\boldsymbol{\lambda}\cdot\mathbf{T}, \quad (3)$$

and mechanical

$$G_{mech} = -\mathbf{T}\cdot\mathbf{sT}, \quad (4)$$

energies. The anisotropy energy originates from magnetic moments having preferred crystallographic directions, ⟨100⟩ and ⟨111⟩ for cubic materials. Rotation of SW particles away from these easy directions requires energy from field, stress, or temperature application. The energy from the field is expressed as the Zeeman energy. Stress contributes energy through the magnetomechanical coupling energy or the strain energy density from magnetostriction as well as through the purely mechanical energy due to the material compliance $\mathbf{s}$, which for Galfenol has cubic symmetry. In Eqs. (3) and (4)

the stress and magnetostriction are treated as vectors where the first three components are longitudinal and the last three shear components. The magnetostriction depends on the SW particle orientation[11]

$$\lambda_i = \frac{3}{2}\lambda_{100}(\theta)m_i^2, \quad i = 1,2,3, \tag{5}$$

$$\lambda_4 = 3\lambda_{111}(\theta)m_1m_2, \tag{6}$$

$$\lambda_5 = 3\lambda_{111}(\theta)m_2m_3, \tag{7}$$

$$\lambda_6 = 3\lambda_{111}(\theta)m_3m_1. \tag{8}$$

The effect of temperature is accounted for through the temperature dependence of the anisotropy coefficients $K_4$ and $K_6$, domain magnetization $M_s$, and magnetostriction coefficients $\lambda_{100}$ and $\lambda_{111}$. For the isothermal processes considered here, these coefficients are constant.

The particle orientation, magnetization **M**, and strain **S** are calculated from the constitutive relations

$$\frac{\partial G}{\partial \mathbf{m}} = 0, \tag{9}$$

$$\mathbf{M} = -\frac{1}{\mu_0}\frac{\partial G}{\partial \mathbf{H}} = M_s\mathbf{m}, \tag{10}$$

$$\mathbf{S} = -\frac{\partial G}{\partial \mathbf{T}} = \boldsymbol{\lambda} + \mathbf{sT}. \tag{11}$$

The minimization (9) is constrained since $|\mathbf{m}|=1$. Analytic solution is not possible because $G$ is a sixth-order function of the particle orientation. There are fourteen possible solutions which correspond to rotation about the six $\langle 100\rangle$ and eight $\langle 111\rangle$ easy directions in response to applied field or stress. Thoelke and Jiles[13] formulated the energy in spherical coordinates and solved for the local minima with iteration. Here the problem is approximately solved in rectangular coordinates, yielding analytic expressions for particle orientation.

First, the constraint is substituted into the Gibbs energy. For example, to find the minimum orientation which lies near the [100] direction, the relation $m_1=\sqrt{1-m_2^2-m_3^2}$ is substituted into the energy so that when $m_2=m_3=0$, the remaining component is the one associated with $m_1=1$. Similarly, to find the local minimum near the $[\bar{1}00]$ direction, the relation $m_1=-\sqrt{1-m_2^2-m_3^2}$ is used so that when $m_2=m_3=0$, the remaining component is the one associated with $m_1=-1$. After this substitution, the two nonlinear equations $\partial G/\partial m_i=0$ are linearized about the easy direction that was used in the substitution of the constraint. Linearization of $\partial G/\partial m_i=0$ about the easy crystal directions is accurate because SW particles are always oriented near an easy crystal direction. If the stress or field rotates a particle far from a particular easy direction it will flip to one of the other thirteen energy equilibria which is closer to an easy direction.

A typical device having a magnetostrictive material consists of a rod in compression with an applied stress sufficiently large to align domains perpendicular to the rod axis.

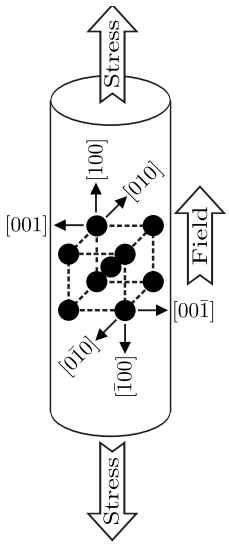


FIG. 2. [100] oriented material where arrows for the field and stress indicate the positive direction which for the stress indicates a tensile load.

An applied magnetic field causes magnetization change and magnetostriction as domains rotate into the applied field direction. At certain critical fields, domains will flip from the current equilibrium to an equilibrium closer to the field direction; in addition, the size of domains in lower energy equilibria will grow at the expense of higher energy domains through domain wall motion. For [100] oriented material (see Fig. 2,) compressive stress at zero field lowers the energy of the four basal plane directions [010], [0$\bar{1}$0], [001], and [00$\bar{1}$]. A sufficient compressive stress will cause all domains to lie in these directions. Applied field rotates these domains into the field direction along the rod. Eventually domain wall motion and domains flipping occurs as the material saturates with all domains oriented in the [100] direction for positive fields and $[\bar{1}00]$ for negative fields.

The SW approximation is accurate when the magnetization process is dominated by domain rotation. This occurs below saturation when sufficient compressive stress has been applied to align all domains in the basal plane. In this case, magnetic field causes magnetization change as domains rotate toward the field. This is calculated with the approximation described previously, linearizing about any of the [010], [0$\bar{1}$0], [001], or [00$\bar{1}$] basal plane directions. Substitution of $m_3=\sqrt{1-m_1^2-m_2^2}$ into $G$ with $H_1=H$, $T_1=T$, and all other inputs zero results in the following after differentiation:

$$\frac{\partial G}{\partial m_1} = 2K_4(m_1 - 2m_1^3 - m_1m_2^2) - 3\lambda_{100}Tm_1 - \mu_0M_sH, \tag{12}$$

$$\frac{\partial G}{\partial m_2} = 2K_4(m_2 - 2m_2^3 - m_2m_1^2), \tag{13}$$

$$\frac{\partial^2 G}{\partial m_1^2} = 2K_4(1 - 6m_1^2 - m_2^2) - 3\lambda_{100}T, \tag{14}$$

$$\frac{\partial^2 G}{\partial m_1 \partial m_2} = -4K_4 m_1 m_2, \tag{15}$$

$$\frac{\partial^2 G}{\partial m_2^2} = 2K_4(1 - 6m_2^2 - m_1^2). \tag{16}$$

The linear approximation of (12) and (13) about $m_1 = m_2 = 0$, the [001] direction, is formulated by

$$\frac{\partial G}{\partial m_1} \approx \left(\frac{\partial G}{\partial m_1}\right)_0 + \left(\frac{\partial^2 G}{\partial m_1^2}\right)_0 m_1 + \left(\frac{\partial^2 G}{\partial m_1 \partial m_2}\right)_0 m_2, \tag{17}$$

$$\frac{\partial G}{\partial m_2} \approx \left(\frac{\partial G}{\partial m_2}\right)_0 + \left(\frac{\partial^2 G}{\partial m_2 m_1}\right)_0 m_1 + \left(\frac{\partial^2 G}{\partial m_2^2}\right)_0 m_2. \tag{18}$$

Substitution from (12)–(16), equating to zero, and solving for $m_1$, the component in the field direction is

$$m_1 = \frac{\mu_0 M_s}{2K_4 - 3\lambda_{100} T} H, \tag{19}$$

hence, the linear susceptibility below saturation is

$$\chi(T) = \frac{\mu_0 M_s^2}{2K_4 - 3\lambda_{100} T}. \tag{20}$$

Relations (19) and (20) are applicable for small rotations about the ⟨100⟩ directions and describe bulk behavior when the material is in a single-domain state. They happen to have the same form of expressions for amorphous materials which by definition are isotropic,[10] with the difference that the material constants here are anisotropic. These nonlinear expressions give a measure of the sensitivity of Galfenol beyond what can be described by the magnetomechanical coupling factor which only applies to linear operating regimes.

## IV. FORCE SENSOR MODEL

The magnetization calculated using the susceptibility (20) is shown with the magnetization measurements in Fig. 3. The model parameters for the $Fe_{79.1}Ga_{20.9}$ sample are $M_s = 970$ kA/m, $\lambda_{100} = 138 \times 10^{-6}$, measured directly from the saturation values of the magnetization and magnetostriction of the 122.7 MPa data set, and $K_4 = 4.98$ kJ/m$^3$, calculated by solving (20) for $K_4$ with the susceptibility and stress values from the 122.7 MPa data set. There is excellent agreement between the model and the measurements except in the lowest stress case [see Fig. 3(a)]. This suggests that 1.38 MPa is not enough stress to fully align domains in the basal plane and hence the magnetization process is not due to domain rotation alone for this stress level. Additionally, the full magnetostriction $(3/2)\lambda_{100}$ (measured with a strain gauge) was not achieved for this data set, providing further evidence that full domain alignment was not achieved.

The model parameters for the $Fe_{81.6}Ga_{18.4}$ sample are $M_s = 1281$ kA/m, $\lambda_{100} = 173 \times 10^{-6}$, measured directly from the saturation values of the magnetization and magnetostriction of the 55.4 MPa data set, and $K_4 = 19.1$ kJ/m$^3$, calculated by solving (20) for $K_4$ with the susceptibility and stress values from the 55.4 MPa data set. Full magnetostriction was achieved for the 27.7 MPa and higher data sets; these measurements are compared with the rotational model in Fig. 3(b). These sets follow the model lines at fields lower than 10 kA/m but diverge rather quickly giving the curves a nonlinear shape. The model comparison for each data set is shown for clarity in separate plots for the $Fe_{81.6}Ga_{18.4}$ sample [see Fig. 3(b)], since increasing stress causes little change in the susceptibility, whereas the data sets for the $Fe_{79.1}Ga_{20.9}$ sample are easily distinguished in the same plot [see Fig. 3(a)].

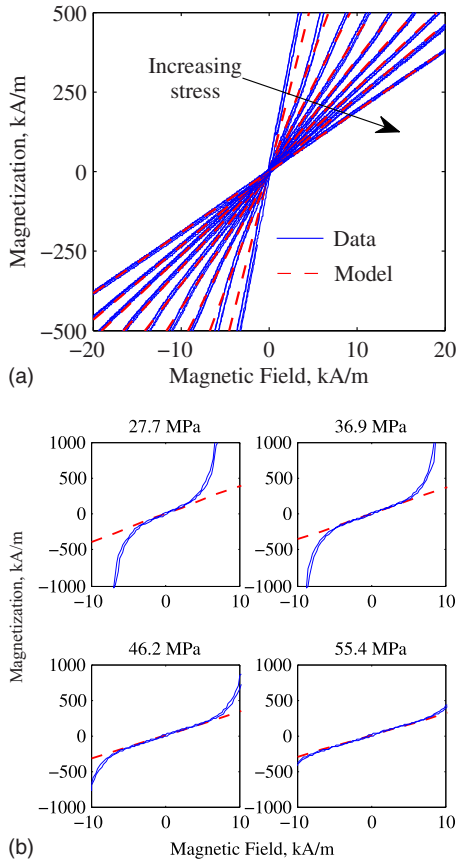


FIG. 3. (Color online) Comparison of rotational model with magnetization measurements of (a) $Fe_{79.1}Ga_{20.9}$ and (b) $Fe_{81.6}Ga_{18.4}$.

There is variability in the reported values of the fourth-order anisotropy constant $K_4$. Noting that $K_4 = -2K_{cubic}$, Restorff *et al.*[7] report values of 28.6, 32.0, and 45.6 kJ/m$^3$ for three different $Fe_{81.6}Ga_{18.4}$ samples. The values are not measured directly but determined from a nonlinear simplex algorithm minimizing the error between an energy averaging model and the data. Rafique *et al.*[14] report 32.5 kJ/m$^3$ for a $Fe_{82}Ga_{18}$ sample. Their work uses the classical approach of numerically integrating the magnetic field over magnetization measurements for two different crystal orientations and assuming that all of the field energy goes to changing the internal energy (assumed to be entirely composed of the anisotropy energy of a rotating SW particle). If the magnetization measurements are carried out over a range including domain flipping or wall motion, this appears as an apparent scaling of the anisotropy constant since all of the field energy is assumed to go toward overcoming anisotropy energy alone. In our approach, a SW model is also used, however, it is only applied in the domain rotation region and is measured

directly from the slope or susceptibility (after directly measuring $M_s$ and $\lambda_{100}$). Both cited works show a trend of decreasing anisotropy with increasing Ga content which agrees with our results. Finally, all three approaches actually measure $K_4+\Delta K_4$ where $\Delta K_4$ is a strain-invariant change in the intrinsic cubic anisotropy due to the magnetoelastic coupling energy.[11]

It is the large difference in anisotropy that results in the different behavior of the differing Ga content samples. Having low anisotropy, the magnetization of the $Fe_{79.1}Ga_{20.9}$ sample is dominated by domain rotation over a large range of fields and stresses. The magnetomechanical coupling (3) dominates the anisotropy energy (1) so that domains which rotate from the basal plane with field application have a large contribution to the bulk magnetization. The linear magnetization versus field region arises from this rotation. Eventually the field energy (2) dominates, causing a nonlinear approach to saturation as domain flipping and wall motion result in the material being composed entirely of domains oriented in the ⟨100⟩ direction aligned with the magnetic field. The denominator of (20) is dominated by the stress term which causes large changes in the susceptibility as the stress is changed. This effect can be used as the basis of a force sensor.

Whereas the magnetization of the $Fe_{79.1}Ga_{20.9}$ sample is dominated by the rotation of a single set of domains, made energetically favorable by the applied stress, the magnetization of the $Fe_{81.6}Ga_{18.4}$ sample is due to the simultaneous rotation of domains from the six ⟨100⟩ and eight ⟨111⟩ easy axes as well as flipping and wall motion of these domains. The larger anisotropy inhibits domain rotation: the field energy goes to domain flipping and wall motion to change the volume fraction of material having domain orientations close to the field direction. The effect of stress in this case is mostly to shift the field location where flipping and wall motion begins, with little change to the rotations. As an illustration, the slope of the domain rotation region is not changed significantly in Fig. 3(b) as stress is increased but the width of the field interval where rotation occurs is increased since stress lowers the energy of domains rotating from the basal plane.

To summarize, the $Fe_{79.1}Ga_{20.9}$ sample is dominated by uniaxial anisotropy imparted by the applied stress and the $Fe_{81.6}Ga_{18.4}$ is dominated by the cubic, magnetocrystalline anisotropy. The result is that the $Fe_{79.1}Ga_{20.9}$ magnetization has large intervals of stress and field which can be accurately modeled by a simple stress dependent susceptibility (20). The $Fe_{81.6}Ga_{18.4}$ sample magnetization has a kinked shape with limited regions dominated by rotation. Description of this behavior requires more complicated models involving statistical distributions of domain orientations[8,15,16] or micromagnetics simulations.[9]

The $Fe_{79.1}Ga_{20.9}$ sample is better suited for use in Galfenol force sensors. The stress sensitivity of its susceptibility in the rotational region is much higher than in the $Fe_{81.6}Ga_{18.4}$ sample (see Fig. 4.) The accurate, low-order, expression for the stress dependence of the susceptibility (20) enables the design and control of transducers. To ensure that the material is used in the domain rotation region, it can be

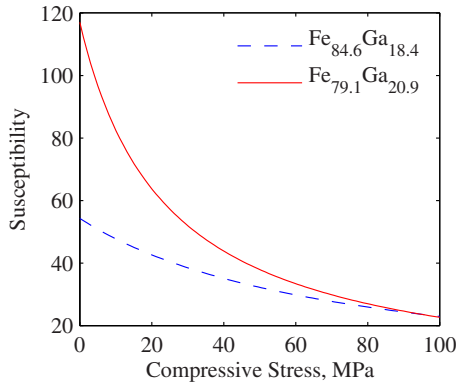


FIG. 4. (Color online) Stress-dependent susceptibility (20) using parameters for the $Fe_{79.1}Ga_{20.9}$ and $Fe_{81.6}Ga_{18.4}$ samples.

stress annealed.[7] Magnetoelastic transducers for force sensing and energy harvesting typically rely on the stress dependence of the magnetic susceptibility.[1] Kleinke and Uras[17] proposed a magnetoelastic force sensor using a transformer made from a magnetostrictive material with an excitation coil on one arm and a detection coil on the other (see Fig. 5). An amplitude modulated signal results and the stress or force is related to the amplitude ratio between the drive and pickup coils. A key advantage of Galfenol for this application is its combination of high magnetostriction and high yield strength. Although the susceptibility is a nonlinear function of stress (20), the relationship between the amplitude ratio and force is linear, even at very high compressive stresses. Furthermore, by using small amplitude magnetic fields centered at zero, the Galfenol behavior is anhysteretic.

The magnetic field $H_e$ produced by the current of the excitation coil sample is controlled and the voltage of the detection coil measured. The force is related to the ratio of the magnetic field and detection voltage. Equations describing the operation of this transducer using Galfenol with cross-section area $A$ can be calculated with (20) and standard magnetic circuit laws. A bias stress or stress annealing and proper selection of the magnetic field amplitude ensures that

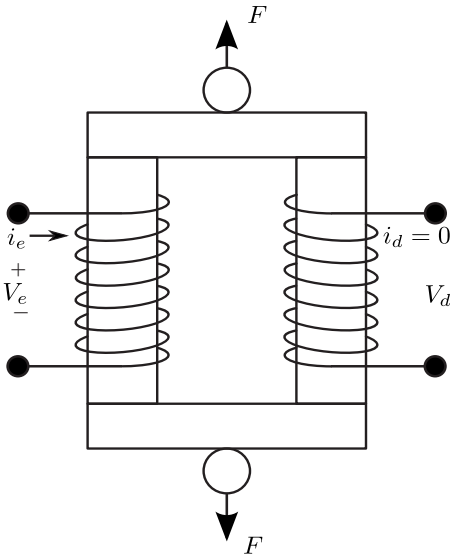


FIG. 5. Force sensor with magnetostrictive core.

the Galfenol sample is operated in the domain rotation region of its magnetization behavior. The detection voltage due to changing flux $\phi$ is found from Faraday's law of induction

$$V_d = -N\frac{d\phi}{dt}, \tag{21}$$

where the detection coil has $N$ turns of wire. From (20) the total magnetic flux through area $A$ is

$$\frac{1}{A\mu_0}\phi = [1+\chi(T)]H_e \approx \chi(T)H_e. \tag{22}$$

The flux due to magnetic field alone can be neglected since $\chi(T) \gg 1$. The detection voltage is then

$$V_d = -\mu_0 NA\left[\chi(T)\frac{dH_e}{dt} + \frac{d\chi(T)}{dT}\frac{dT}{dt}H_e\right]. \tag{23}$$

By using an excitation field with a frequency $\omega_e$ much greater than the frequency of the force, the second term in the square brackets can be neglected. The amplitude of the detection voltage $\bar{V}_d$ is then related to the magnetic field amplitude $\bar{H}_e$ by

$$\bar{V}_d = \mu_0 NA\omega_e\chi(T)\bar{H}_e. \tag{24}$$

The $Fe_{79.1}Ga_{20.9}$ sample has a higher susceptibility which is more sensitive to stress changes (see Fig. 4), giving a higher detection voltage. From (20), the susceptibility can be increased by decreasing the anisotropy $K_4$ or increasing the saturation magnetization $M_s$. The sensitivity to stress changes can be increased by increasing the magnetostriction $\lambda_{100}$. Magnetostriction measurements have been reported for Ga concentrations of 0–35 at. % with peaks occurring at 19 and 27 at. %.[18] Anisotropy constants have been separately reported for Ga concentrations of 0–20 at. % (Ref. 14) and 12.5–22 at. % with a trend of decreasing anisotropy for increasing Ga concentration. The saturation magnetization has also been reported to decrease with Ga concentration but by much lower factors than the anisotropy. Ideally, the anisotropy coefficient $K_4$ should be slightly greater than zero. A negative value would result in the need for a higher bias stress to prealign domains in the basal plane, since in this case the [100] directions are not easy directions. Given the variability and low resolution of reported anisotropy values, it is difficult to accurately select the ideal Ga concentration. However, the trends suggest the optimal value lies between the magnetostriction peak of 19 at. % and the anisotropy sign change value of around 22 at. %.

Using a higher magnetic field frequency and amplitude also gives a higher detection voltage. Substitution from (20) and solution for the force $F=2AT$ gives

$$F = -\frac{2}{3}\frac{N(A\mu_0 M_s)^2\omega_e}{\lambda_{100}}\left(\frac{\bar{H}_e}{\bar{V}_d}\right) + \frac{4AK_4}{3\lambda_{100}}. \tag{25}$$

The force is linearly related to the amplitude ratio $\bar{H}_e/\bar{V}_d$ by known material and geometric properties.

Employing the $Fe_{79.1}Ga_{20.9}$ sample, the difference between the maximum expected tensile stress and the bias or internal compressive stress should not exceed 18 MPa. In addition, the excitation field amplitude should be less than 5 kA/m. These limits ensure the accuracy of (25) by keeping the magnetization process in the domain rotation region.

## V. CONCLUDING REMARKS

Magnetization measurements of $Fe_{79.1}Ga_{20.9}$ and $Fe_{81.6}Ga_{18.4}$ are linear with magnetic field in certain intervals of stress and magnetic field. These regions arise from coherent rotation of domains from the basal plane and occur when a sufficient compressive stress aligns domains in the four easy crystal directions of the basal plane at zero magnetic field. The slope of the linear region is proportional to the field energy and inversely proportional to the anisotropy and magnetomechanical coupling energies. Energy minimization can be used to interpret the differences in the magnetization processes of the two samples. Magnetization of $Fe_{81.6}Ga_{18.4}$ is more strongly influenced by domain flipping and wall motion due to its higher anisotropy impeding domain rotation. As a result, its magnetization versus field curves at constant stress have a distinctive kinked shape whereas the $Fe_{79.1}Ga_{20.9}$ curves are largely linear until saturation, having lower anisotropy which permits more domain rotation. The susceptibility of the $Fe_{79.1}Ga_{20.9}$ sample is more sensitive to stress. The stress dependence of the susceptibility in the linear or domain rotation region of both samples is accurately modeled with a simple expression derived from energy minimization. This expression motivates the use of Galfenol with Ga concentrations having high magnetostriction and saturation magnetization with a small, positive fourth-order anisotropy constant for transducers utilizing stress dependent susceptibility. This expression also shows that despite the nonlinear stress dependence of the susceptibility, a linear force transducer can be constructed with a transformer made from Galfenol. This study has identified a sensing principle, operating regime, and composition for Galfenol-based force sensing. Future work will investigate specific device geometries and signal conditioning.

## ACKNOWLEDGMENTS

We wish to acknowledge the financial support by the Office of Naval Research, MURI grant No. N000140610530. We also thank Jim Restorff and Marilyn Wun-Fogle at the Naval Surface Warfare Center, Carderock Division for providing the Galfenol measurements.

[1] M. J. Dapino, Struct. Eng. Mech. **17**, 303 (2004).
[2] A. E. Clark, J. B. Restorff, M. Wun-Fogle, T. A. Lograsso, and D. L. Schlagel, IEEE Trans. Magn. **36**, 3238 (2000).
[3] X. Tan and J. S. Baras, Automatica **40**, 1469 (2004).
[4] D. C. Jiles and J. B. Thoelke, J. Magn. Magn. Mater. **134**, 143 (1994).
[5] W. D. Armstrong, J. Magn. Magn. Mater. **263**, 208 (2003).
[6] R. C. Smith and M. J. Dapino, IEEE Trans. Magn. **42**, 1944 (2006).
[7] J. B. Restorff, M. Wun-Fogle, A. E. Clark, and K. B. Hathaway, IEEE Trans. Magn. **42**, 3087 (2006).
[8] P. G. Evans and M. J. Dapino, IEEE Trans. Magn. **44**, 1711 (2008).
[9] J. X. Zhang and L. Q. Chen, Acta Mater. **53**, 2845 (2005).
[10] M. Wun-Folge, H. T. Savage, and A. E. Clark, Sens. Actuators, A **12**, 323 (1987).
[11] C. Kittel, Rev. Mod. Phys. **21**, 541 (1949).
[12] F. Liorzou, B. Phelps, and D. L. Atherton, IEEE Trans. Magn. **36**, 418 (2000).
[13] J. B. Thoelke and D. C. Jiles, J. Magn. Magn. Mater. **104–107**, 1453

(1992).
[14]S. Rafique, J. R. Cullen, M. Wuttig, and J. Cui, J. Appl. Phys. **95**, 6939 (2004).
[15]J. Atulasimha, G. Akhras, and A. B. Flatau, J. Appl. Phys. **103**, 07B336 (2008).
[16]P. G. Evans and M. J. Dapino, J. Appl. Phys. **107**, 063906 (2010).
[17]D. K. Kleinke and H. M. Uras, Rev. Sci. Instrum. **65**, 1699 (1994).
[18]A. E. Clark, K. B. Hathaway, M. Wun-Fogle, J. B. Restorff, T. A. Lograsso, J. M. Keppins, G. Petculescu, and R. A. Taylor, J. Appl. Phys. **93**, 8621 (2003).